Pramana – J. Phys. (2017) 89:52
DOI 10.1007/s12043-017-1451-7

Phenomenological study of Z' in the minimal $B - L$ model at LHC

K M BALASUBRAMANIAM[1,2]

[1]Department of Physics and Astronomy, University of Sussex, Brighton BN1 9QH, UK
[2]Theory Division, Physical Research Laboratory, Navrangpura, Ahmedabad 380 009, India
E-mail: kmbala86@gmail.com

Published online 5 October 2017

Abstract. The phenomenological study of neutral heavy gauge boson (Z'_{B-L}) of the minimal $B-L$ extension was done in the context of the LHC, on the dimuon production channel. The study begins with the LEP-II constraints on Z' searches, and the dimuon events are simulated at the parton level at CM energies of 7 TeV and 8 TeV and studied with an integrated luminosity of 1.21 fb^{-1} and 20.5 fb^{-1} respectively. Later, the ATLAS detector-specific cuts unique to the muon pairs are imposed followed by the signal selection cuts on the invariant mass of the dimuon which restrict the events that are to be passed for signal-background analysis, that are finally compared with the ATLAS data, and accounted for no experimental detection of Z'_{B-L} boson. It has been simulated further at 14 TeV CM energy with an integrated luminosity of 300 fb^{-1} to predict a possible discovery of this $B - L$ neutral-heavy gauge boson with a mass corresponding to 1.5 TeV and a Z' coupling strength of 0.2 based on the signal-background analysis.

Keywords. Dataset-specific parameters; LEP-II constraints; detector-specific kinematic cuts; signal-specific kinematic cuts; Z'_{B-L} boson; heavy resonance; dimuon production channel; LHC; ATLAS.

PACS Nos 12.60.Cn; 12.60.Fr; 13.38.Dg; 13.85.Lg; 14.70.Hp; 14.70.Pw; 14.80.Bn; 14.80.Fd; 12.15.Ji; 11.80.Cr; 11.30.Fs

1. Introduction

We study the Z'_{B-L} detection prospects at the LHC in the dimuon final state by carrying out a parton level simulation. The Drell–Yan process, $pp \to \mu^+\mu^-$ (at tree level) simulated in the $B - L$ model (mediated by γ, Z, Z'_{B-L}, h_1 (SM Higgs) and h_2 ($B - L$ model Higgs)) forms the signal-plus-background, whereas the SM process (mediated by γ, Z and h (SM Higgs)) forms the background-alone. We have done the signal-background analysis in studying the potential for Z'_{B-L} discovery in the Large Hadron Collider (LHC).

1.1 *Outline of the study*

A brief introduction to the minimal $B - L$ model is given in §2 covering the details on the $B-L$ Lagrangian (2.2) and the spontaneous breaking of the $B - L$ symmetry with the gauge boson spectrum (2.3). In §3, the mechanics of this study are explained: starting from the phenomenological tools (3.1) to the study of Z'_{B-L} confidence level (CL) of a possible case (3.4.1) and ruling out the sisters' categories of the reviewed case by comparing with the ATLAS experimental bounds (3.4.2). Lastly, we conclude by making remarks on the studied cases (4) and catch a glimpse of other experimentally ruled out cases (figures 6–10) that are involved in this research.

2. Theoretical framework

2.1 *The $B - L$ model*

The $B - L$ model is a triply-minimal extension of the Standard Model (SM) in the gauge, scalar and fermion sectors. As the gauge sector of the SM is extended by a single $U(1)$ factor related to baryon minus lepton ($B - L$) number, the $B - L$ gauge sector becomes minimal. Similarly, the requirement of a complex scalar singlet for the spontaneous breaking of $B - L$ symmetry makes the scalar sector as minimal. Thirdly, the introduction of a SM-singlet right-handed (RH) fermion per generation to eliminate the triangular $B-L$ gauge anomalies makes the fermion sector minimally

extended. The $B-L$ charge is chosen to cure the new gauge and mixed $U(1)$ gravitational anomalies [1–4].

2.2 *The Lagrangian of the minimal $B-L$ model*

The Lagrangian of the minimal $B-L$ model obeying the $SU(3)_C \otimes SU(2)_L \otimes U(1)_Y \otimes U(1)_{B-L}$ gauge symmetry can be decomposed as [1]

$$\mathcal{L} = \mathcal{L}_{\rm S} + \mathcal{L}_{\rm YM} + \mathcal{L}_{\rm f} + \mathcal{L}_{\rm Y}, \tag{1}$$

where the terms on the RHS are the scalar, Yang–Mills (YM)/gauge, fermion and Yukawa parts respectively.

2.2.1 *Scalar sector.*

For the spontaneous breaking of $B-L$ symmetry of the extra $U(1)$ gauge group, a complex scalar singlet (χ) is introduced along with the SM scalar doublet (Φ). Thus, the scalar Lagrangian becomes

$$\mathcal{L}_{\rm S} = (D^\mu \Phi)^\dagger (D_\mu \Phi) + (D^\mu \chi)^\dagger (D_\mu \chi) - V(\Phi, \chi)$$

with the scalar potential given by

$$\begin{aligned} V(\Phi,\chi) &= m^2 \Phi^\dagger \Phi + \mu^2 |\chi|^2 \\ &\quad + (\Phi^\dagger \Phi \;\; |\chi|^2) \begin{pmatrix} \lambda_1 & \lambda_3/2 \\ \lambda_3/2 & \lambda_2 \end{pmatrix} \begin{pmatrix} \Phi^\dagger \Phi \\ |\chi|^2 \end{pmatrix} \\ &= m^2 \Phi^\dagger \Phi + \mu^2 |\chi|^2 + \lambda_1 (\Phi^\dagger \Phi)^2 \\ &\quad + \lambda_2 |\chi|^4 + \lambda_3 \Phi^\dagger \Phi |\chi|^2, \end{aligned}$$

where Φ and χ are the complex scalar Higgs doublet and singlet fields. For Φ and χ fields, the $B-L$ charges are taken as 0 and +2 respectively. The charge of the χ field has been chosen to ensure the gauge invariance of the fermion sector of the minimal $B-L$ model.

2.2.2 *Yang–Mills/gauge sector.*

The non-Abelian field strengths of this model are the same as in the SM whereas the Abelian ones can be written as follows:

$$\mathcal{L}_{\rm YM}^{\rm Abel} = -\frac{1}{4} F^{\mu\nu} F_{\mu\nu} - \frac{1}{4} F'^{\mu\nu} F'_{\mu\nu},$$

where

$$F_{\mu\nu} = \partial_\mu B_\nu - \partial_\nu B_\mu,$$
$$F'_{\mu\nu} = \partial_\mu B'_\nu - \partial_\nu B'_\mu.$$

The fields B_μ and B'_ν are the $U(1)_Y$ and $U(1)_{B-L}$ gauge fields respectively. In this field basis, the covariant derivative is

$$\begin{aligned} D_\mu &\equiv \partial_\mu + i g_S T^\alpha G^\alpha_\mu + i g T^\alpha W^\alpha_\mu \\ &\quad + i g_1 Y B_\mu + i(\tilde{g} Y + g'_1 Y_{B-L}) B'_\mu. \end{aligned}$$

The gauge couplings $\tilde{g}$ and g'_1 are free parameters. The pure $B-L$ model is defined by the condition $\tilde{g} = 0$ (i.e., the free parameter $\tilde{g}$ is nullified at the EW scale). This implies that there is no mixing at the tree level between the Z' bosons of $B-L$ model and the Z bosons of the SM.

2.2.3 *Fermion sector.*

The fermion Lagrangian density (with k being the generation index) is given by

$$\begin{aligned} \mathcal{L}_{\rm f} = \sum_{k=1}^{3} & (i \bar{q}_{kL} \gamma_\mu D^\mu q_{kL} + i \bar{q}_{kR} \gamma_\mu D^\mu q_{kR} \\ & + i \bar{d}_{kR} \gamma_\mu D^\mu d_{kR} + i \bar{l}_{kL} \gamma_\mu D^\mu l_{kL} \\ & + i \bar{e}_{kR} \gamma_\mu D^\mu e_{kR} + i \bar{\nu}_{kR} \gamma_\mu D^\mu \nu_{kR}), \end{aligned}$$

where the fields' charges are the usual SM and $B-L$ ones (in particular, $B-L = 1/3$ for quarks and -1 for leptons with no distinction between generations, hence ensuring universality). The $B-L$ charge assignments of the fields as well as the introduction of new fermion RH heavy neutrinos (ν_R's, charged -1 under $B-L$) are designed to eliminate the triangular $B-L$ gauge anomalies of the theory.

Therefore, the $B-L$ gauge extension of the SM gauge group broken at the TeV scale necessarily requires at least one new scalar field and three new fermion fields which are charged with respect to the $B-L$ group.

2.2.4 *Yukawa sector.*

Finally, the Yukawa interactions are

$$\begin{aligned} \mathcal{L}_Y = \sum_{i,\,j,\,k\,=\,1}^{3} \Big(& - y^d_{jk} \bar{q}_{jL} d_{kR} \Phi \; - \; y^u_{jk} \bar{q}_{jL} u_{kR} \tilde{\Phi} \\ & - y^e_{jk} \bar{l}_{jL} e_{kR} \Phi \; - \; y^\nu_{jk} \bar{l}_{jL} \nu_{kR} \tilde{\Phi} \\ & - y^M_{jk} (\overline{\nu}_R)^c_j \nu_{kR} \chi \Big) \; + \; h.c., \end{aligned}$$

where $\tilde{\Phi} = i\sigma^2 \Phi^*$ and the last term is the Majorana contribution, and the others are the usual Dirac ones. While working on the basis in which the RH neutrino Yukawa coupling matrices y^M are diagonal, real and positive, these are the only allowed gauge invariant terms. The last term in the above equation combines the neutrinos to the new scalar singlet field χ which allows the dynamical generation of neutrino masses, and acquires a VEV through the Higgs mechanism.

2.3 *Spontaneous breaking of $B-L$ symmetry and gauge boson spectrum*

In the Feynman gauge, the scalar fields (Φ and χ) can be parametrized [1] and [2] as

$$\Phi = \frac{1}{2} \begin{pmatrix} -i(\omega^1 - i\omega^2) \\ v + (h + iz) \end{pmatrix},$$
$$\chi = \frac{1}{\sqrt{2}} (x + (h' + iz')),$$

where v is the SM's vacuum expectation value (VEV), x is the $B-L$ model's VEV, $\omega^{\pm}=\omega^1\mp i\omega^2$, z and z' are the would-be Goldstone bosons of $W^{\pm}$, Z and Z' respectively.

$$D^{\mu}\Phi(D_{\mu}\Phi)^{\dagger}=\frac{1}{2}(\partial^{\mu}h)(\partial_{\mu}h)+\frac{1}{8}(h+v)^2[g^2|W_1^{\mu}-iW_2^{\mu}|^2+(gW_3^{\mu}-g_1B^{\mu}-\tilde{g}B'^{\mu})^2]$$

and

$$D^{\mu}\chi(D_{\mu}\chi)^{\dagger}=\frac{1}{2}(\partial^{\mu}h')(\partial_{\mu}h')+\frac{1}{2}(h'+x)^2(g_1'2B'^{\mu})^2,$$

where we have taken $Y_{\chi}^{B-L}=2$ to guarantee the gauge invariance of the Yukawa terms (2.2.4). In the first of the above two equations, we can immediately recognize the SM charged gauge bosons $W^{\pm}$, with $M_W=gv/2$ as in the SM. The other gauge boson masses are not so simple to identify, because of mixing. In analogy with the SM, the fields of definite mass are linear combinations of B^{μ}, W_3^{μ} and B'^{μ}. The explicit expressions are

$$\begin{pmatrix}B^{\mu}\\W_3^{\mu}\\B'^{\mu}\end{pmatrix}=X\begin{pmatrix}A^{\mu}\\Z^{\mu}\\Z'^{\mu}\end{pmatrix},$$

where

$$X=\begin{pmatrix}\cos\vartheta_{\omega} & -\sin\vartheta_{\omega}\cos\vartheta' & \sin\vartheta_{\omega}\sin\vartheta'\\ \sin\vartheta_{\omega} & \cos\vartheta_{\omega}\cos\vartheta' & -\cos\vartheta_{\omega}\sin\vartheta'\\ 0 & \sin\vartheta' & \cos\vartheta'\end{pmatrix},$$

with $-\pi/4\le\vartheta'\le\pi/4$, such that

$$\tan 2\vartheta'=\frac{2\tilde{g}\sqrt{g^2+g_1^2}}{\tilde{g}^2+16(\frac{x}{v})^2g_1'^2-g^2-g_1^2}.$$

The gauge boson masses are

$$M_A=0. \tag{2}$$

Now, setting $\tilde{g}$ to 0 for the pure $B-L$ model, the mixing angle ϑ' vanishes, implying no mixing, at the tree level, between the $Z_{\rm SM}$ and Z'_{B-L} bosons. The Z and Z'_{B-L} masses are

$$M_Z=\sqrt{g^2+g_1^2}\cdot\frac{v}{2}, \tag{3}$$

$$M_{Z'_{B-L}}=2g_1'x. \tag{4}$$

To complement the section on the $B-L$ model, we summarize the mass eigenstates and the assignation of hypercharge (Y) and $B-L$ quantum number ($B-L$) to the chiral fermionic and scalar fields in tables 1 and 2 respectively.

Table 1. Mass eigenstates [1].

Name	Quarks	Leptons	Neutrinos	Higgses
ψ	q	l	ν_l and ν_h	h_1 and h_2
Mass	m_q	m_l	m_{ν_l} and m_{ν_h}	m_{h_1} and m_{h_2}

Table 2. Hypercharge (Y) and $B-L$ quantum number assignation to chiral fermion and scalar fields [1].

ψ	q_L	u_R	d_R	l_L	e_R	ν_R	Φ	χ
$SU(3)_C$	3	3	3	1	1	1	1	1
$SU(2)_L$	2	1	1	2	1	1	2	1
Y	$\frac{1}{6}$	$\frac{2}{3}$	$-\frac{1}{3}$	$-\frac{1}{2}$	-1	0	$\frac{1}{2}$	0
$B-L$	$\frac{1}{3}$	$\frac{1}{3}$	$\frac{1}{3}$	-1	-1	-1	0	2

3. Z'_{B-L} – Analysis and results

3.1 *Phenomenological tools*

We have done the search for Z' boson in the context of the LHC on the dimuon production channel, $pp\to\mu^+\mu^-$ by employing the FeynRules model file for the minimal $B-L$ model, implemented by Basso and Pruna [5]. The motivation was to get myself introduced to the techniques of FeynRules [6]. We used FeynRules2.0 [7] and Mathematica (version-9) [8] to generate the Universal FeynRules Output (UFO) [9] files which were fed into the event generator, MadGraph5.0 [10]. We have used the in-built parton density function (PDF) set, CTEQ6L1 in MadGraph5.0 [10] in our study and employed MadAnalysis5 [11] for signal-background analysis. We have resorted to the standard Large Electron Positron (LEP)-II experimental bounds [12] on Z' searches as shown in figure 1 to standardize the values of the parameters for our study.

3.2 *Initialization of Z'_{B-L} parameters*

We have chosen the values of Z' coupling constant (g_1') as 0.2 and 0.5 with four different masses ($M_{Z'}$ in TeV) parameters of values, 1.5, 2.0, 3.0, and 5.0 respectively in accordance with the bounds from the LEP-II experiment.

The expression for the partial decay widths of Z'_{B-L} into SM fermions ($\Gamma_{Z'\to f\bar{f}}$) has been derived from the coupling vertex of Z'_{B-L} with the SM fermions is

$$\Gamma_{Z'\to f\bar{f}}=\frac{M_{Z'}}{12\pi}C_f(v^f)^2\left[1+2\frac{m_f^2}{M_{Z'}^2}\right]\sqrt{1-\frac{4m_f^2}{M_{Z'}^2}},$$

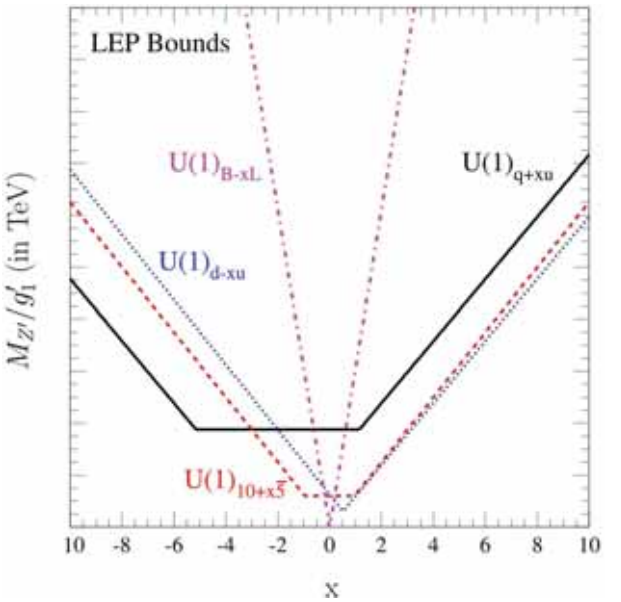

Figure 1. LEP-II constraints [12] on $M_{Z'}/g'_1$ of various Z' models. For the arbitrary parameter, x = 1 (i.e., for the $B-L$ model), only $M_{Z'}/g'_1 \geq 6$ TeV are allowed.

Table 3. The dataset-specific parameters, viz., mass ($M_{Z'}$), coupling of Z'_{B-L} with SM fermions (g'_1) and the total decay width of Z'_{B-L} into SM fermions ($\Gamma_{Z'}$) upon which this study is based. C : the Z' signal with $M_{Z'} =$ 3000 GeV, $g'_1 = 0.2$ and $\Gamma_{Z'} = 76.39$ GeV, Nil: The discarded datasets with parameters $g'_1 = 0.5$ with $M_{Z'} = 1.5$ and 2.0 TeV, as their LHE files got corrupted.

$M_{Z'}$ (in GeV)	$\Gamma_{Z'}$ (in GeV) for $g'_1 = 0.2$	$\Gamma_{Z'}$ (in GeV) for $g'_1 = 0.5$
1500	38.20 A	Nil
2000	50.93 B	Nil
3000	76.39 C	477.45 D
5000	127.32 E	795.75 F

where C_f is the colour factor of the fermion (f), v^f ($= (B-L)g'_1$) is the coupling between the $B-L$ charge of fermion (f) and Z' coupling between SM fermions (g'_1) and m_f is the mass of fermion (f). The total decay width ($\Gamma_{Z'}$) of the Z'_{B-L} boson is the sum of all the partial decay widths ($\Gamma_{Z'\to f\bar{f}}$) of Z'_{B-L} into SM-fermion pairs except the neutrino pairs (taking the SM-neutrinos as massless). These sets of parameters are grouped into six datasets as shown in table 3.

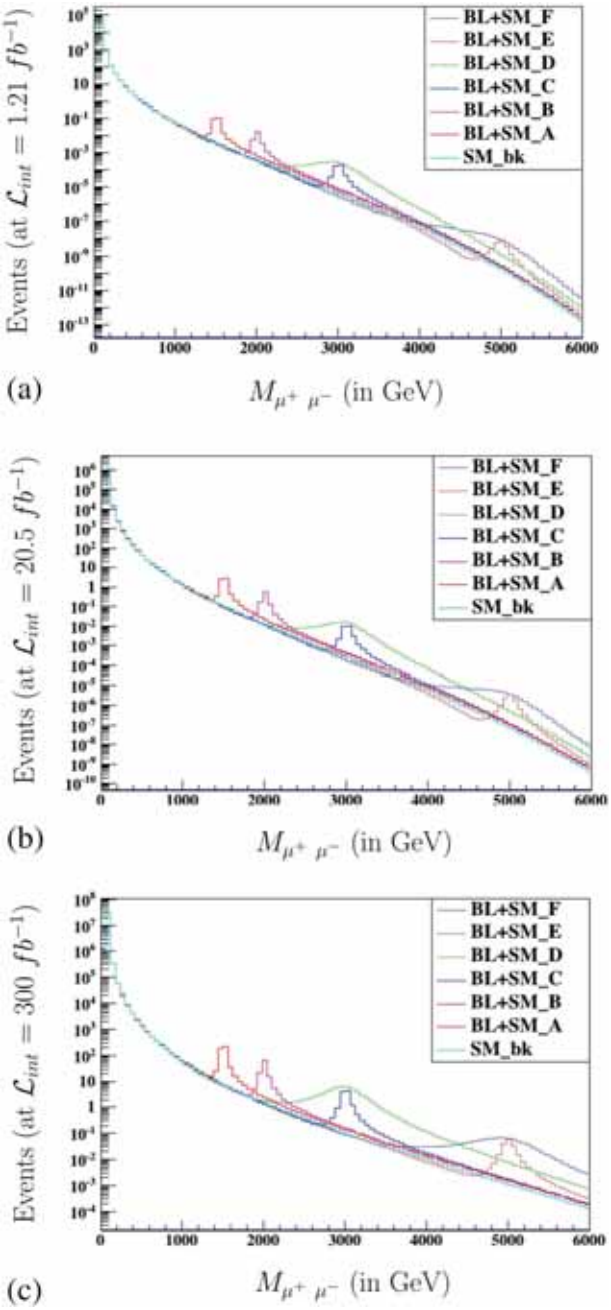

Figure 2. Z'_{B-L} resonances in the process, $pp \to \mu^+\mu^-$ for the considered datasets (signal + background) and dataset SM (background alone) without any kinematic cuts. The event distributions of all the seven datasets are superimposed one upon the other. The resonance of the SM's Z boson at $M_{\mu^+\mu^-} = 91.18$ GeV can be seen very close to 0 GeV of $M_{\mu^+\mu^-}$. (**a**) Simulated events at 7 TeV CM energies, (**b**) simulated events at 8 TeV CM energies and (**c**) simulated events at 14 TeV CM energies.

Initially, the $B-L$ model (in the form of UFO [9] files) has been imported into the MadGraph5.0's [10] environment and the process $pp \to \mu^+\mu^-$ is generated. Then, the dataset-specific parameters are set in the created process directory to produce one million partonic-level

Table 4. Signal-specific kinematic cuts on the studied datasets (with signal+background).

$\Gamma_{\text{SW}}^{\text{signals}}$	Signal-specific kinematic cuts (same for CM energies of 7, 8 and 14 TeV)
$\Gamma_{\text{SW}}^{\text{signal}-\text{B}}$	923.6 GeV $\leq M_{\mu^+\mu^-} \leq$ 3076.4 GeV
$\Gamma_{\text{SW}}^{\text{signal}-\text{C}}$	1385.4 GeV $\leq M_{\mu^+\mu^-} \leq$ 4614.6 GeV
$\Gamma_{\text{SW}}^{\text{signal}-\text{D}}$	783.8 GeV $\leq M_{\mu^+\mu^-} \leq$ 5216.2 GeV
$\Gamma_{\text{SW}}^{\text{signal}-\text{E}}$	2309.0 GeV $\leq M_{\mu^+\mu^-} \leq$ 7691.0 GeV
$\Gamma_{\text{SW}}^{\text{signal}-\text{F}}$	1306.4 GeV $\leq M_{\mu^+\mu^-} \leq$ 8693.6 GeV

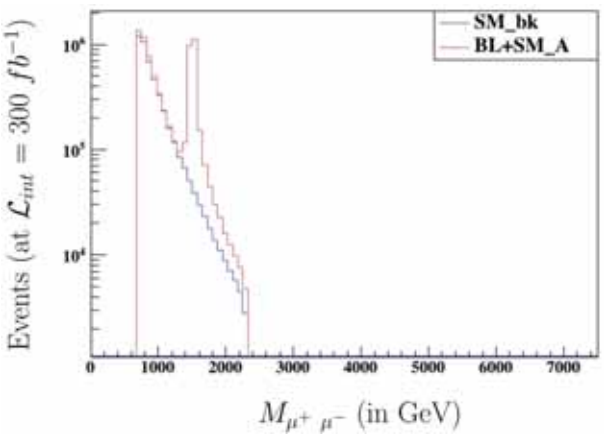

Figure 3. Event distributions for datasets A and SM at 14 TeV after cuts on P_{T}, η and $M_{\mu^+\mu^-}$ with Z'_{B-L} signal with CL of 9.5σ at $M_{\mu^+\mu^-} = 1.5$ TeV ($M_{Z'}^{\text{dataset}-\text{A}}$) and $g'_1 = 0.2$.

events at the centre of mass (CM) energy of 7 TeV, per each invariant mass (of charged lepton pairs) window of varied sizes. These windows are to ensure no loss of any significant events across the whole range of simulation which has spanned across the entire invariant mass range, 0–7000 GeV of the final-state muon pairs. The format of the simulated events in compliant with the Les Houches Event Accord (LHEA) [13] was generated as the Les Houches Event (LHE) [13] files.

LHE files corresponding to each invariant mass window were fed into MadAnalysis5 [11] where they got joined into a single large LHE [13] file corresponding to a particular dataset, which encompasses the entire simulation range of width, approximately 6000–7000 GeV of muon pairs' invariant mass.

3.3 *Comparison of 7, 8 and 14 TeV simulated events of all the datasets*

At this juncture, the obtained single LHE file of massive size was normalized with an integrated luminosity of 1.21 fb^{-1}. The whole machinery of §3.1 was repeated for the remaining datasets. All of these datasets are an admixture of Z'_{B-L} signal and the SM background. For the analysis of Z'_{B-L} signal from the background, another LHE file of large size has been generated as previously for the SM process. This generation was done by importing the default model SM in the MG5 environment and the events are simulated for the dimuon production from proton–proton collisions with the same PDF set, CTEQ6L1.

The distribution of events vs. the invariant mass of muon pairs is shown in figure 2a at the CM energy of 7 TeV with an integrated luminosity of $\mathcal{L}_{\text{int}} = 1.21$ fb^{-1}. We have repeated similar study with the collision energy of 8 TeV and 14 TeV and normalized the generated partonic-level events with an integrated luminosity of $\mathcal{L}_{\text{int}} = 20.5$ fb^{-1} and $\mathcal{L}_{\text{int}} = 300.0$ fb^{-1} respectively. The event distribution with the muon pairs' invariant mass for the two cases just discussed is shown in figures 2b and 2c.

We shall observe an increase in the total number of events as we move from the event distributions studied at CM energies of 7 TeV to 8 TeV and then to 14 TeV respectively. The events corresponding to all the datasets are colour coded distinctly in all the detailed figures. The signal peaks become prominent with increasing collision energy and integrated luminosity, which is very conspicuous in figures 2a, 2b and 2c. This variation in the signal's prominence shall be accounted for a potential discovery of Z'_{B-L} in the upcoming sections.

The event distributions shown in figure 2 have six Z'_{B-L} signal peaks corresponding to the signal-plus-background datasets, and one peak at $M_{\mu^+\mu^-} = 91.18$ GeV corresponding to the SM Z-resonance where the six signal-plus-background datasets (viz., A, B, C, D, E and F) coincide with the background-alone dataset (dataset SM).

3.4 *Signal vs. background analysis for Z'_{B-L} resonance in datasets A and SM*

The LHE files of dataset A and the dataset SM generated at 14 TeV CM energy were fed into MadAnalysis5 [11] environment and normalized to an integrated luminosity of $\mathcal{L}_{\text{int}} = 300$ fb^{-1}.

Table 5. Selected and rejected events after the kinematic cuts on final-state muon pairs for the datasets A and SM at 14 TeV pp collisions.

	Events retained ($K \pm \delta K$)	Events rejected ($R \pm \delta R$)
Dataset A (signal + background)		
No cut	35351789 ± 10184.5	Nil
$P_T > 20.0$ GeV	26308333 ± 9352	9043456 ± 4033
$\eta < 2.4$	26294016 ± 9348	14317 ± 119
692.7 GeV $\leq M_{\mu^+\mu^-} \leq$ 2307.3 GeV	1126.2 ± 33.6	26292890 ± 9347
Dataset SM (background alone)		
No cut	35527829 ± 10662.1	Nil
$P_T > 20.0$ GeV	26949438 ± 9895	8578391 ± 3971
$\eta < 2.4$	26935139 ± 9890	14298 ± 119
692.7 GeV $\leq M_{\mu^+\mu^-} \leq$ 2307.3 GeV	807.6 ± 28.4	26934331 ± 9890

Then, two ATLAS detector-specific kinematic cuts were applied on the transverse momenta ($P_T > 20.0$ GeV) and pseudorapidity ($\eta < 2.4$) of the final-state muon pairs and the events satisfying these cuts were selected for further study. We have calculated the cumulative efficiency (which is a ratio between the selected events and the sum of the selected and the rejected events) after the cuts and checked that it is never greater than one, to ensure that we did not lose any significant events with these cuts.

The signal-specific kinematic cuts (common for studies done at 7, 8 and 14 TeV CM energies) on the invariant mass ($M_{\mu^+\mu^-}$) have been chosen as a sampling window (SW) with width (Γ_{SW}) as

$$\Gamma_{SW}^{signal-A} = M_{Z'}^{signal-A} \pm 3\Gamma_{Z'}^{signal-A}. \quad (5)$$

Thus, for dataset A, with $M_{Z'}^{signal-A} = 1500$ GeV and $\Gamma_{Z'}^{signal-A} = 38.20$ GeV, the signal-specific cuts can be implemented by selecting the events whose invariant mass falls within the range,

$$692.7 \text{ GeV} \leq M_{\mu^+\mu^-} \leq 2307.3 \text{ GeV} (\text{for } \Gamma_{SW}^{signal-A}).$$

The signal-specific kinematic cuts on $M_{\mu^+\mu^-}$ corresponding to the width of the sampling windows of the remaining datasets viz., B, C, D, E and F are given in table 4.

The event distribution with the muon pairs' invariant mass for dataset A, at 14 TeV collision energy is shown in figure 3. By repeating the procedures mentioned earlier, the event distributions for dataset A, at 7 TeV and 8 TeV were obtained which are shown in figures 4a and 5a respectively.

The confidence level (CL)/statistical significance of the Z'_{B-L} signal has been calculated using

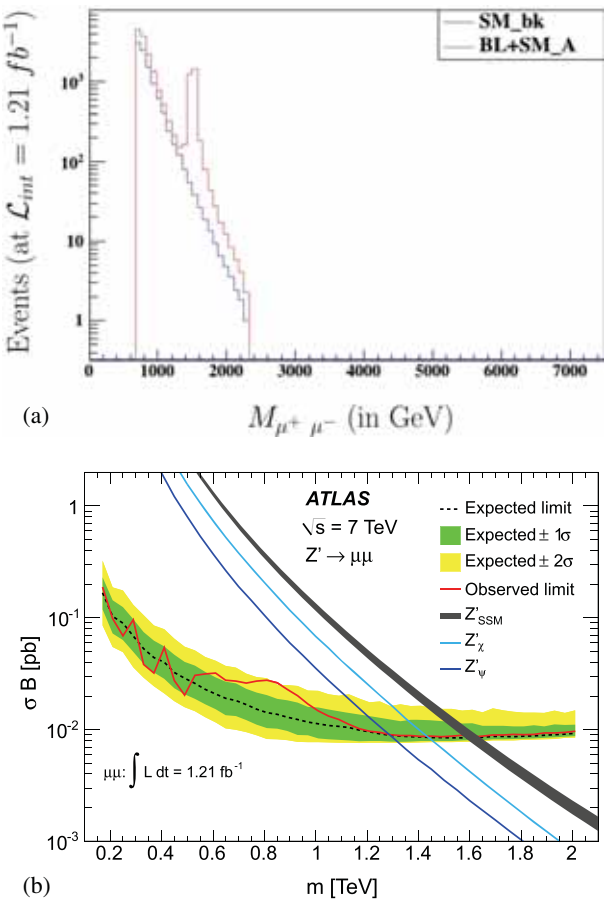

Figure 4. Comparison between datasets A and SM with ATLAS searches on the neutral heavy resonance at 7 TeV pp collisions with $\mathcal{L}_{int} = 1.21$ fb^{-1}. (**a**) Event distribution of datasets A and SM at 7 TeV collisions with Z'_{B-L} signal of 0.1σ significance and (**b**) variation of cross-section with invariant mass; ATLAS searches on Z' in dimuon channel at 7 TeV collision with an integrated luminosity ($\mathcal{L}_{int}$) of 1.21 fb^{-1} [14] with no singularity at $M_{\mu^+\mu^-} = 1.5$ TeV.

$$K_{signal} = K_A - K_{SM},$$

$$\text{Signals CL} = \frac{K_{signal}}{\sqrt{K_{signal} + K_{background}}}.$$

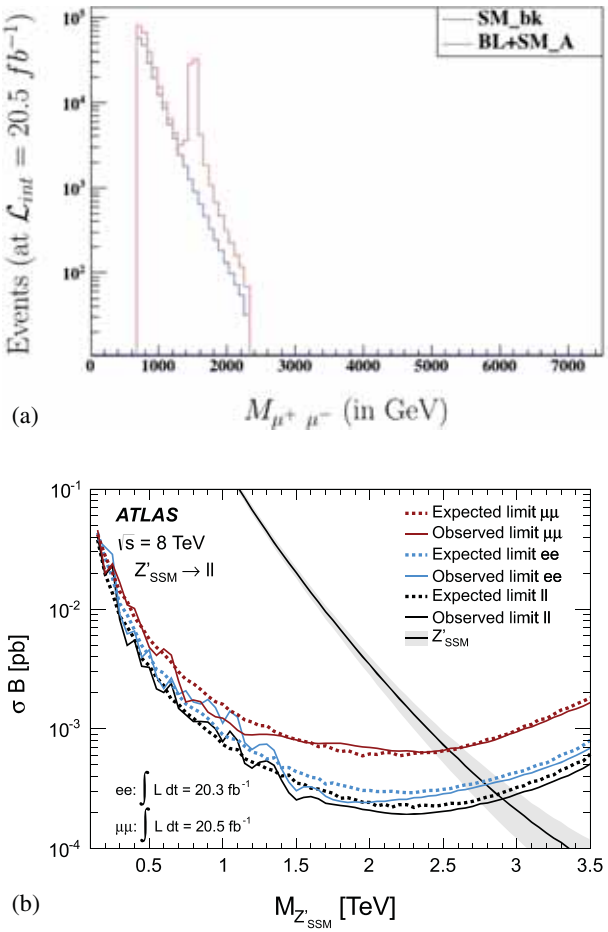

Figure 5. Comparison between datasets A and SM with ATLAS searches on the neutral heavy resonance at 8 TeV pp collisions with $\mathcal{L}_{\text{int}} = 20.5$ fb^{-1}. (**a**) Event distribution for datasets A and SM at 8 TeV collisions with the Z'_{B-L} signal of 0.8σ significance and (**b**) variation of cross-section with invariant mass; ATLAS searches on Z' in dimuon channel at 8 TeV collision with an integrated luminosity ($\mathcal{L}_{\text{int}}$) of 20.5 fb^{-1} [15] with no resonance at $M_{\mu^+\mu^-} = 1.5$ TeV.

3.4.1 *Confidence level of the signal in dataset A at 14 TeV collision energy.* We have studied the confidence level of Z'_{B-L} signal of the dataset A at 14 TeV with an integrated luminosity of $\mathcal{L}_{\text{int}} = 300$ fb^{-1}. The event distributions with the invariant mass for datasets A and SM at 14 TeV CM energy are shown in figure 3. The number of events selected for signal-background analysis after the application of three successive kinematic cuts on the datasets that are just discussed, in the same order is listed in table 5.

The CL of Z'_{B-L} signal has been calculated to be 9σ which accounts for a possible experimental discovery.

3.4.2 *Comparison of datasets A and SM at 7 and 8 TeV collisions with respective ATLAS results.* The dataset A studied at 7 TeV collision energy has been compared with the ATLAS experimental bounds on the searches of Z' in the dimuon channel at 7 TeV LHC collisions with an integrated luminosity ($\mathcal{L}_{\text{int}}$) of 1.21 fb^{-1} [14]. The CL of the signal in the dataset A, at 7 TeV collision is 0.1σ, which is merely a statistical fluctuation as shown in figure 4a. We have confirmed with the ATLAS results of 7 TeV pp collisions at 1.5 TeV where the cross-section is continuous with no signal peak, corresponding to the solid red line, titled 'Observed limit' in figure 4b.

A similar comparison between figures 5a and 5b has been made to confirm Z'_{B-L} resonance with CL of 0.8σ in the dataset A, at 8 TeV pp collision corresponds to no experimental possibility. This detection impossibility is indicated by the continuous solid red line without any singularity, captioned with 'Observed limit $\mu\mu$' in figure 5b [15].

4. Conclusion

Thus, with the signal significance (CL) of 9σ for dataset A at 14 TeV CM energy with $\mathcal{L}_{\text{int}} = 300$ fb^{-1}, this study predicts a potential discovery of the heavy neutral gauge boson (Z'_{B-L}) corresponding to the dataset A with a mass $M_{Z'}$ of 1.5 TeV and a Z' coupling strength g'_1 of 0.2 with the SM fermions at the LHC as in figure 3.

The comparative study between the datasets A and SM with the ATLAS experimental searches on heavy resonances at 7 and 8 TeV on the dimuon channel confirms the non-observance of any Z' boson. And this comparison validates our study of Z'_{B-L} signal with CL of 0.1σ and 0.8σ at 7 and 8 TeV collisions of datasets A and SM respectively as in figures 4 and 5.

Acknowledgements

This study of Z'_{B-L} was carried out as a dissertation thesis of M.Sc. Particle Physics programme, under the guidance of Dr Sebastian Jäger, University of Sussex, UK. The author expresses his sincere thanks and gratitude to his thesis adviser. He would like to thank the Physical Research Laboratory (PRL), Ahmedabad for hospitality and support during which he got an opportunity to present this work in the Pheno01@IISERMohali workshop. He is grateful to the organisers of Pheno01@IISERMohali workshop for supporting his stay at the IISER-Mohali, India. The final part of this work in preparing the manuscript was done during his visiting tenure in Harish-Chandra Research Institute (HRI), India. The author is extending his sincere gratitude to Prof. Biswarup Mukhopadhyaya, and the Regional Centre for Accelerator-based Particle Physics (RECAPP)-HRI for supporting him and his learning process.

Appendix A: Comparison of 7, 8 and 14 TeV simulated datasets

The event distribution of the remaining datasets studied at 7, 8 and 14 TeV are compared in this Appendix (figures 6, 7, 8, 9 and 10 corresponding to datasets B, C, D, E and F respectively). All the cases of Appendix A correspond to experimentally ruled out possibilities as the confidence level (CL) of all the cases are less than 3σ.

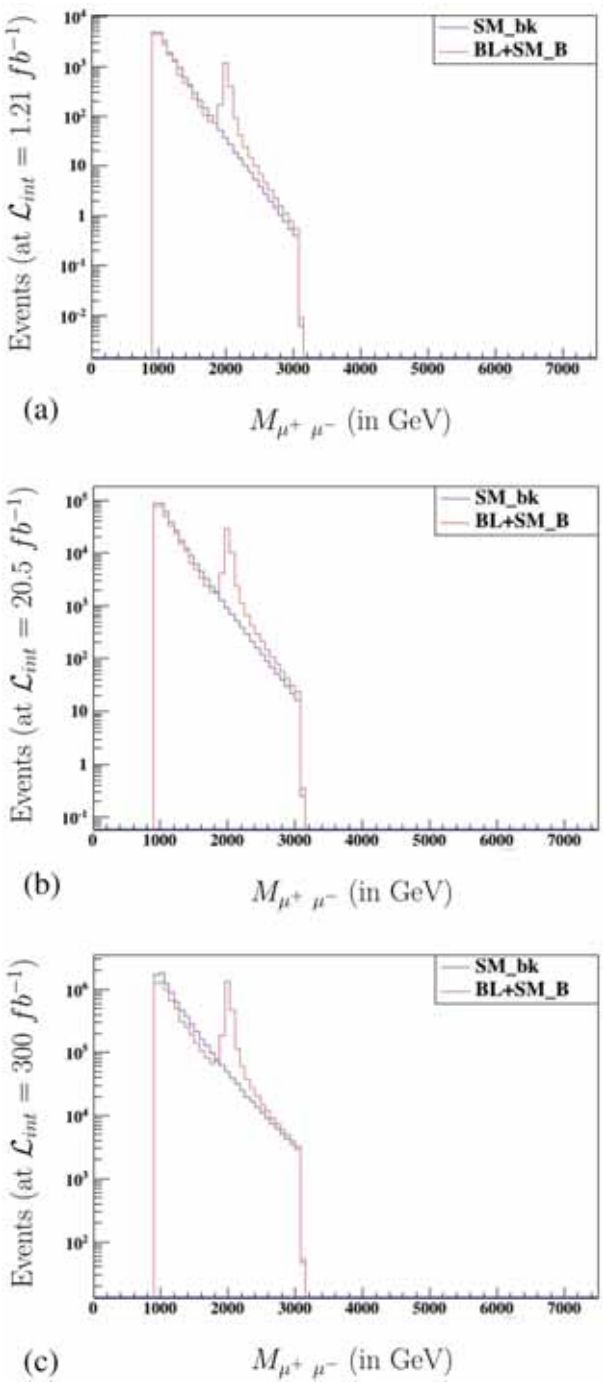

Figure 6. Dataset B with cuts, $P_T > 20.0$ GeV, $\eta < 2.4$ and 923.6 GeV $\leq M_{\mu^+\mu^-} \leq$ 3076.4 GeV (for $\Gamma_{SW}^{signal-B}$) at (**a**) $\sqrt{s} = 7$ TeV with CL $< 1\sigma$, (**b**) $\sqrt{s} = 8$ TeV with CL $= 0.2\sigma$ and (**c**) $\sqrt{s} = 14$ TeV with CL $= 4.3\sigma$.

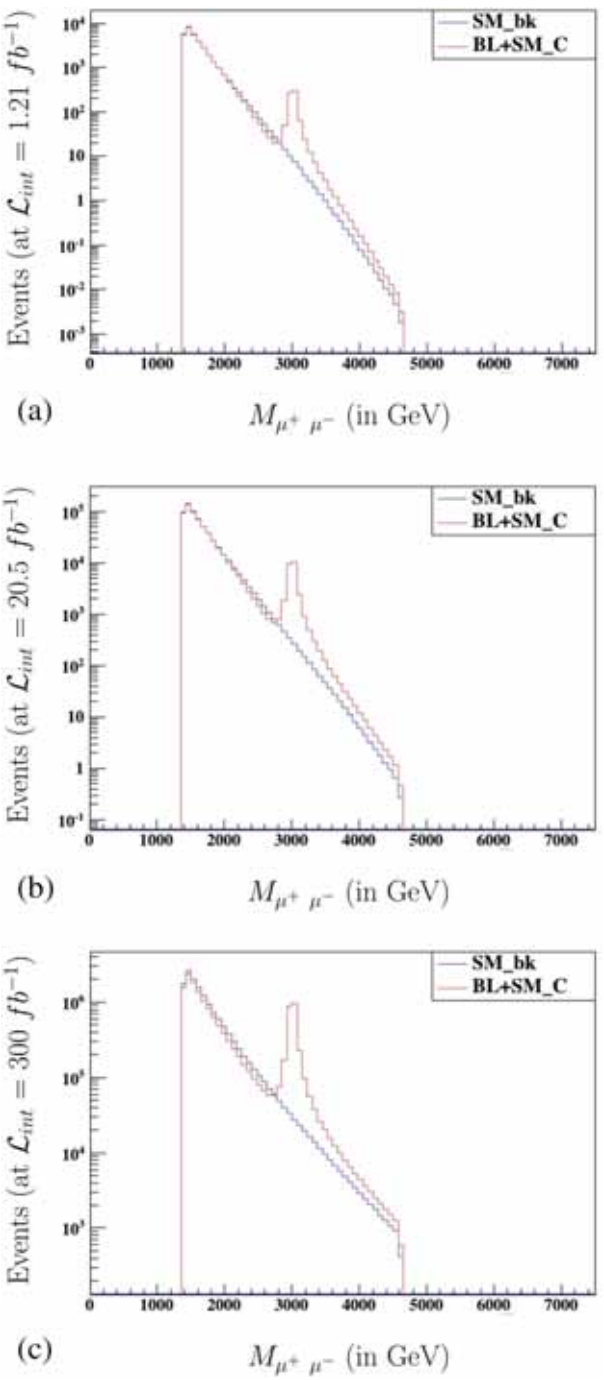

Figure 7. Dataset C with cuts, $P_T > 20.0$ GeV, $\eta < 2.4$ and 1385.4 GeV $\leq M_{\mu^+\mu^-} \leq$ 4614.6 GeV (for $\Gamma_{SW}^{signal-C}$) at (**a**) $\sqrt{s} = 7$ TeV with CL $< 1\sigma$, (b) $\sqrt{s} = 8$ TeV with CL $\ll 1\sigma$ and (**c**) $\sqrt{s} = 14$ TeV with CL $= 1\sigma$.

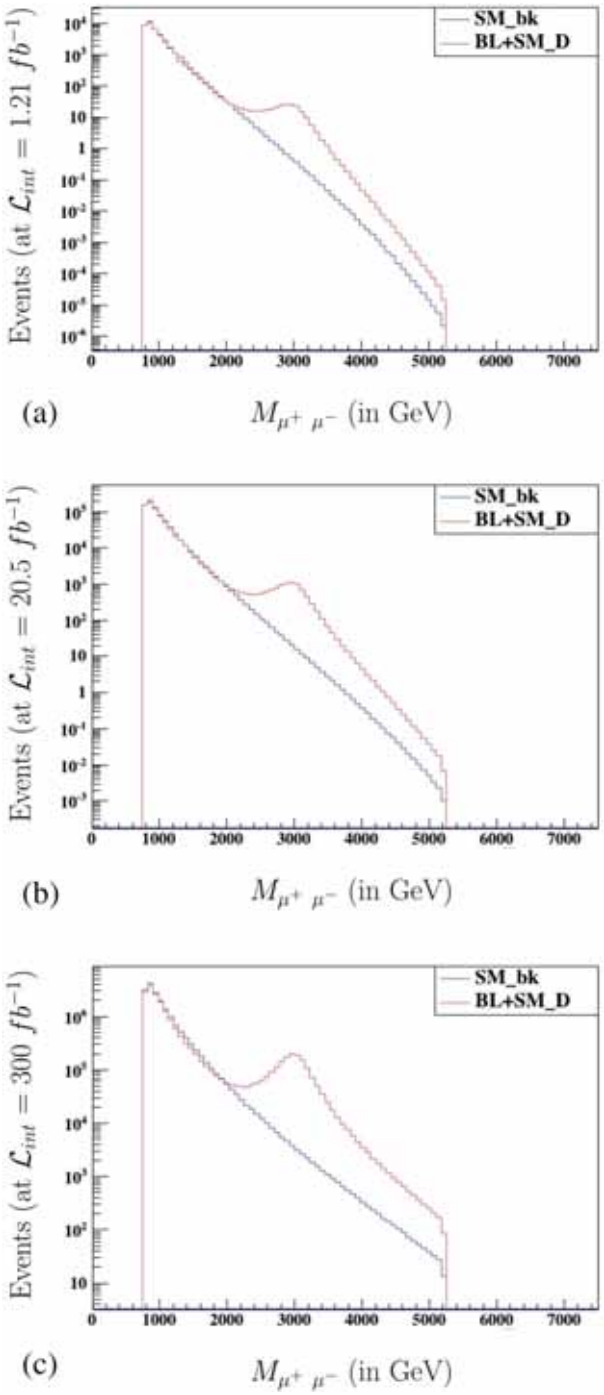

Figure 8. Dataset D with cuts, $P_T > 20.0$ GeV, $\eta < 2.4$ and 783.8 GeV $\leq M_{\mu^+\mu^-} \leq$ 5216.2 GeV (for $\Gamma_{\rm SW}^{\rm signal-D}$) at (**a**) $\sqrt{s} = 7$ TeV with CL $< 1\sigma$, (**b**) $\sqrt{s} = 8$ TeV with CL $\ll 1\sigma$ and (**c**) $\sqrt{s} = 14$ TeV with CL $= 0.7\sigma$.

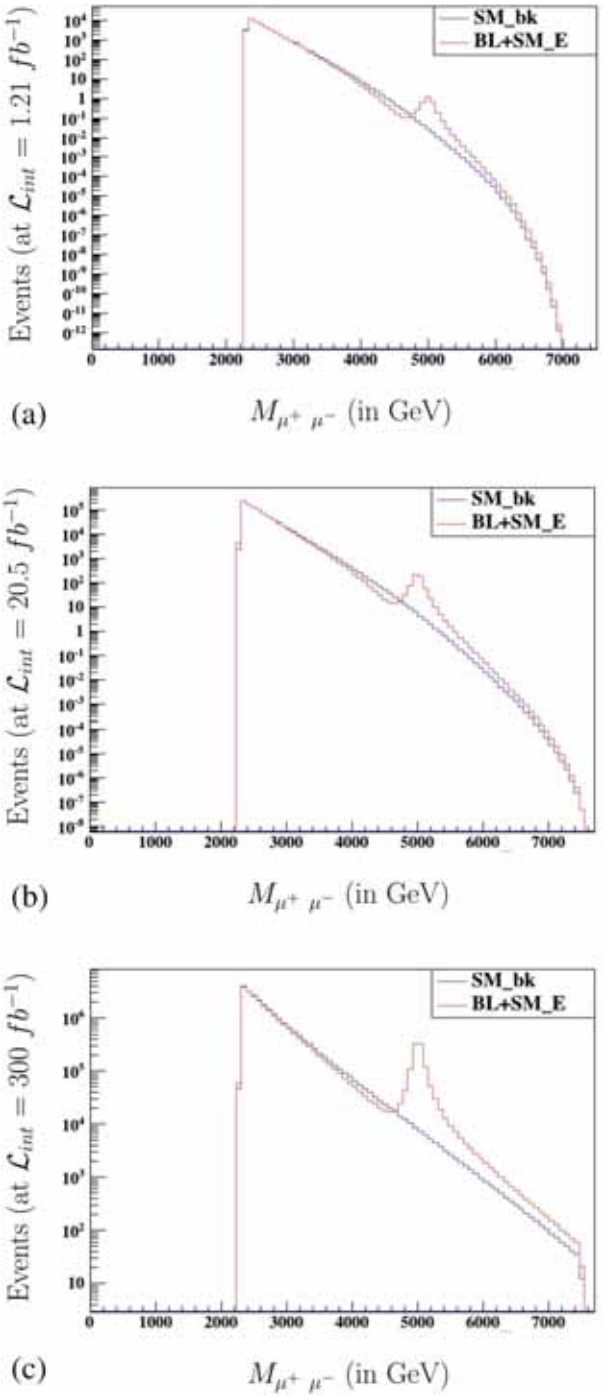

Figure 9. Dataset E with cuts, $P_T > 20.0$ GeV, $\eta < 2.4$ and 2309.0 GeV $\leq M_{\mu^+\mu^-} \leq$ 7691.0 GeV (for $\Gamma_{\rm SW}^{\rm signal-E}$) at (**a**) $\sqrt{s} = 7$ TeV with CL $< 1\sigma$, (**b**) $\sqrt{s} = 8$ TeV with CL $\ll 1\sigma$ and (**c**) $\sqrt{s} = 14$ TeV with CL $= 0\sigma$.

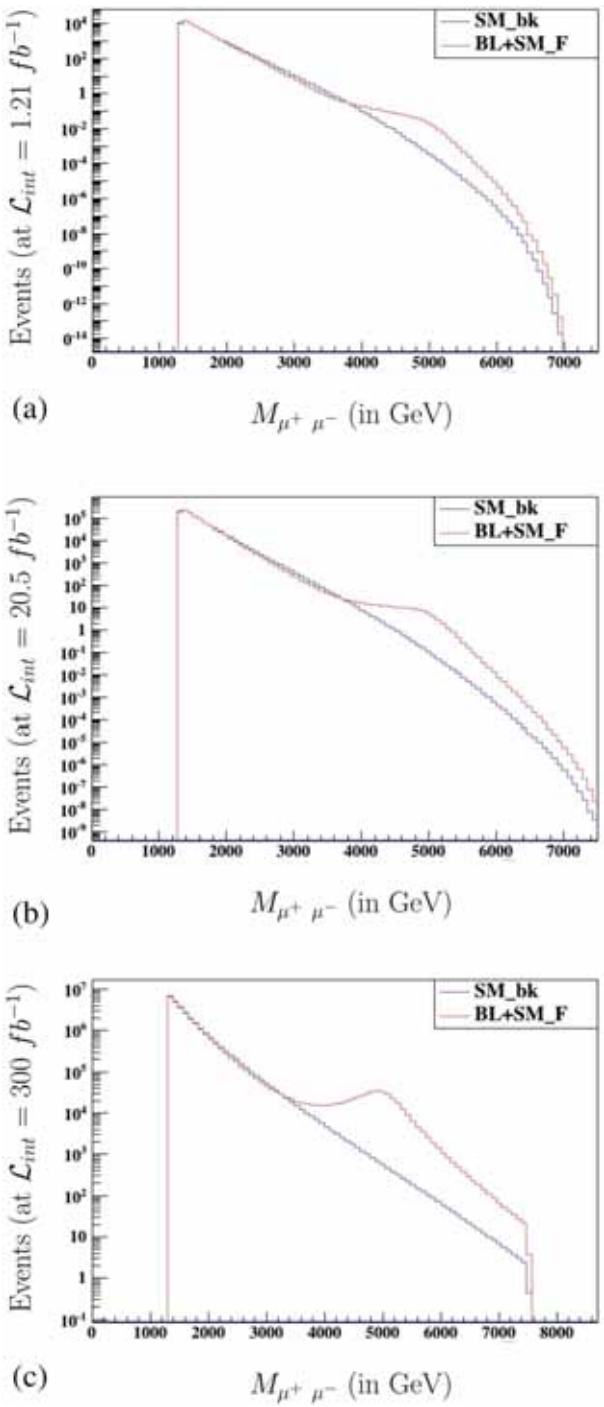

Figure 10. Dataset F with cuts, $P_T > 20.0$ GeV, $\eta < 2.4$ and 1306.4 GeV $\leq M_{\mu^+\mu^-} \leq$ 8693.6 GeV (for $\Gamma_{SW}^{signal-F}$) at (**a**) $\sqrt{s} = 7$ TeV with CL $< 1\sigma$, (**b**) $\sqrt{s} = 8$ TeV with CL $\ll 1\sigma$ and (**c**) $\sqrt{s} = 14$ TeV with CL $\ll 1\sigma$.

References

[1] L Basso, arXiv:1106.4462 [hep-ph]

[2] A Biswas, S Choubey and S Khan, *J. High Energy Phys.* **1608**, 114 (2016), doi:10.1007/JHEP08(2016)114, arXiv:1604.06566 [hep-ph]

[3] M Klasen, F Lyonnet and F S Queiroz, arXiv:1607.06468 [hep-ph]

[4] A Alves, A Berlin, S Profumo and F S Queiroz, *J. High Energy Phys.* **1510**, 076 (2015), doi:10.1007/JHEP10(2015)076, arXiv:1506.06767 [hep-ph]

[5] L Basso and G M Pruna, https://feynrules.irmp.ucl.ac.be/attachment/wiki/B-L-SM/B-L.fr

[6] N D Christensen and C Duhr, *Comput. Phys. Commun.* **180**, 1614 (2009), doi:10.1016/j.cpc.2009.02.018, arXiv:0806.4194 [hep-ph]

[7] A Alloul, N D Christensen, C Degrande, C Duhr and B Fuks, doi:10.1016/j.cpc.2014.04.012, arXiv:1310.1921 [hep-ph]

[8] S Wolfram, Wolfram Research, Inc., Mathematica, Version 9.0, Champaign, IL (2012), https://www.wolfram.com/mathematica/new-in-9/

[9] C Degrande, C Duhr, B Fuks, D Grellscheid, O Mattelaer and T Reiter, *Comput. Phys. Commun.* **183**, 1201 (2012), doi:10.1016/j.cpc.2012.01.022, arXiv:1108.2040 [hep-ph]

[10] J Alwall *et al*, *J. High Energy Phys.* **1407**, 079 (2014), doi:10.1007/JHEP07(2014)079, arXiv:1405.0301 [hep-th]

[11] E Conte, B Fuks and G Serret, *Comput. Phys. Commun.* **184**, 222 (2013), doi:10.1016/j.cpc.2012.09.009, arXiv:1206.1599 [hep-ph]

[12] M Carena, A Daleo, B A Dobrescu and T M P Tait, *Phys. Rev. D* **70**, 093009 (2004), doi:10.1103/PhysRevD.70.093009, arXiv:hep-ph/0408098

[13] J Alwall *et al*, *Comput. Phys. Commun.* **176**, 300 (2007), doi:10.1016/j.cpc.2006.11.010, arXiv:hep-ph/0609017

[14] ATLAS Collaboration: G Aad *et al, Phys. Rev. Lett.* **107**, 272002 (2011), doi:10.1103/PhysRevLett.107.272002, arXiv:1108.1582 [hep-ex]

[15] ATLAS Collaboration: G Aad *et al*, *Phys. Rev. D* **90(5)**, 052005 (2014), doi:10.1103/PhysRevD.90.052005, arXiv:1405.4123 [hep-ex]

[16] J Alwall, M Herquet, F Maltoni, O Mattelaer and T Stelzer, *J. High Energy Phys.* **1106**, 128 (2011), doi:10.1007/JHEP06(2011)128, arXiv:1106.0522 [hep-ph]

[17] L Basso, A Belyaev, S Moretti and G M Pruna, *J. Phys. Conf. Ser.* **259**, 012062 (2010), doi:10.1088/1742-6596/259/1/012062, arXiv:1009.6095 [hep-ph]

[18] L Basso, S Moretti and G M Pruna, *J. Phys. G* **39**, 025004 (2012), doi:10.1088/0954-3899/39/2/025004, arXiv:1009.4164 [hep-ph]

[19] C W Chiang, N D Christensen, G J Ding and T Han, *Phys. Rev. D* **85**, 015023 (2012), doi:10.1103/PhysRevD.85.015023, arXiv:1107.5830 [hep-ph]

[20] R Contino, *Nuovo Cimento B* **123**, 511 (2008), doi:10.1393/ncb/i2008-10553-3, arXiv:0804.3195 [hep-ph]

[21] F Del Aguila, *Acta Phys. Polon. B* **25**, 1317 (1994), arXiv:hep-ph/9404323

[22] A Kundu and B Mukhopadhyaya, *Int. J. Mod. Phys. A* **11**, 5221 (1996), doi:10.1142/S0217751X9600239X, arXiv:hep-ph/9507305

[23] P Langacker, *Adv. Ser. Direct. High Energy Phys.* **14**, 15 (1995), doi:10.1142/9789814503662_0002, arXiv:hep-ph/0304186
[24] P Langacker, *Rev. Mod. Phys.* **81**, 1199 (2009), doi:10.1103/RevModPhys.81.1199, arXiv:0801.1345 [hep-ph]
[25] T G Rizzo, *AIP Conf. Proc.* **542**, 152 (2000), doi:10.1063/1.1336251, arXiv:hep-ph/0001140
[26] J D Lykken, eConf C **960625**, NEW140 (1996), arXiv:hep-ph/9610218
[27] T G Rizzo, arXiv:hep-ph/0610104
[28] M Perelstein, doi:10.1142/9789814327183_0008, arXiv:1002.0274 [hep-ph]
[29] N Okada and S Okada, *Phys. Rev. D* **93(7)**, 075003 (2016), doi:10.1103/PhysRevD.93.075003, arXiv:1601.07526 [hep-ph]
[30] Yu Ya Komachenko and M Yu Khlopov, *Yadernaya Fizika* (1990) **51**, 1081 (1990), [English translation: *Sov. J. Nucl. Phys.* **51(4)**, 692 (1990)]
[31] S Banerjee, M Mitra and M Spannowsky, *Phys. Rev. D* **92(5)**, 055013 (2015), doi:10.1103/PhysRevD.92.055013, arXiv:1506.06415 [hep-ph]